

Mergers Fall Short: Non-merger Channels Required for Galactic Heavy Element Production

Muhammed Saleem,^{1,*} Hsin-Yu Chen,^{1,†} Daniel M. Siegel,^{2,3} Philippe Landry,⁴ Jocelyn S. Read,⁵ and Kaile Wang¹

¹*Department of Physics, The University of Texas at Austin, 2515 Speedway, Austin, TX 78712, USA*

²*Institute of Physics, University of Greifswald, D-17489 Greifswald, Germany*

³*Department of Physics, University of Guelph, Guelph, Ontario N1G 2W1, Canada*

⁴*Stripe, Toronto, ON M5J 1T1, Canada*

⁵*Department of Physics, California State University Fullerton, Fullerton, CA, USA*

(Dated: September 5, 2025)

Since the discovery of the binary neutron star merger GW170817 and its associated kilonova, neutron star mergers have been established as a key production channel for r -process elements in the Universe. However, various evidences, including the observations of r -process abundances as inferred from stellar spectra of Milky Way disk stars, suggest that additional channels are needed to fully account for the r -process element enrichment in the Milky Way. Neutron star–black hole mergers and fast-merging binary neutron star systems are among the leading alternative candidates. In this paper, we combine gravitational-wave observations from LIGO–Virgo–KAGRA with data from short gamma-ray bursts, Galactic pulsars, and Galactic [Eu/Fe] versus [Fe/H] abundance observations to assess the contribution of these mergers to r -process enrichment in the Galactic disk. We find that neither neutron star–black hole mergers nor fast-merging binary neutron star populations can serve as the dominant additional channel without generating strong tension with existing observations and theoretical expectations. These results constrain the viable sources of Galactic r -process enrichment and underscore the necessity of non-merger production channels.

I. INTRODUCTION

The origins of the heaviest elements in the Universe via rapid neutron capture (r -process) nucleosynthesis remains a key question in astrophysics. While it is known that the r -process happens in neutron-rich environments [1, 2], their dominant astrophysical sites are still debated. Compact binary mergers, particularly binary neutron star (BNS) mergers, have been recognized as promising sources of r -process elements [3–5]. The detection of GW170817 and its associated kilonova provided direct evidence for r -process nucleosynthesis in BNS mergers [6–8]. However, the relative role of BNS mergers compared to other potential channels, such as neutron star–black hole (NSBH) mergers [9, 10], magnetorotational supernovae [11, 12], collapsars [13], and giant flares from magnetars [14, 15] is an open problem. For example, recent chemical evolution studies have raised concerns about whether the event rate evolution of BNS mergers are consistent with the early enrichment seen in metal-poor stars in the Milky Way [16–22]. Similar concerns and conclusions are derived from chemical evolution studies of (ultra-faint) dwarf galaxies and globular clusters [23–28].

One of the observational probes of r -process enrichment in the Milky Way is the relationship between [Eu/Fe] and [Fe/H] (where $[A/B] \equiv \log_{10}(N_A/N_B) - \log_{10}(N_A/N_B)_{\odot}$; N denotes number abundances and \odot denotes solar), which traces the evolution of europium (Eu, a representative r -process element) relative to iron

(Fe) as the Galaxy chemically evolves. Observations of metal-poor stars, particularly in the Galactic halo and thick disk, reveal a significant presence of Eu even at low [Fe/H] [29, 30], indicating that r -process production was already occurring in the early history of the Galaxy. In order to match the early enrichment, at least some events must occur promptly after star formation—an argument supported by stars like J1521–3538, an extremely r -process-enhanced star with [Eu/Fe] = +2.2 and [Fe/H] \sim –3 [31]. The relative abundance of Eu decreases at higher metallicities, implying an increase in late-time Fe production and/or decrease in Eu enrichment. These trends—particularly the negative slope in the [Eu/Fe] versus [Fe/H] relation observed in Milky Way disk stars—place stringent constraints on the rates and yields (mass of r -process elements produced per event) of r -process sources throughout cosmic history. Using [Eu/Fe]–[Fe/H] evolution as a reference, one can test whether the proposed astrophysical sites can reproduce the chemical evolution history of the Milky Way.

In our recent study [32], we investigated whether BNS mergers alone can account for the observed r -process enrichment of disk stars in the Milky Way ([Fe/H] \gtrsim –1). Standard BNS (“delayed BNS” henceforth) formation scenario predicts a delay relative to the star formation rate (SFR) [33, 34]. We modeled Eu production from BNS mergers using a one-zone galactic chemical evolution model [35] that incorporates models of star formation history from X-ray observations [36], delay-time distributions constrained by short gamma-ray burst (sGRB) observations [37], event rates and mass distribution constrained by gravitational-wave (GW) observations [38, 39], neutron star equation-of-state (EOS) constraints by GW and pulsar observations [40], and semi-

* muhammed.cholayil@austin.utexas.edu

† hsinyu@austin.utexas.edu

analytical fits to numerical simulations of BNS mergers for event yields [41]. The study found that, to explain the observed abundance trends, BNS mergers would need to occur with a delay-time distribution of power-law index $\alpha \leq -2.0$ and minimum delay time $t_{\min} \leq 40$ Myr at 90% confidence (following the delay-time model in Eq. 2 of [37]), contrasting those inferred from sGRBs [37, 42, 43]. If BNS mergers were assumed to follow the sGRB-inferred delays, an additional enrichment channel is necessary. The study concluded that this additional channel must track the SFR closely and likely contribute a dominant part (45 – 95% at 90% confidence) of the Eu yield in the Galaxy. Similar conclusions were also found in [16, 21].

Following these conclusions, it becomes essential to explore other potential contributors to the r -process. NSBH mergers and fast-merging BNS are two strong candidates among the discussion. There have been studies on r -process contributions from NSBH systems under various mass and spin configurations [44, 45]. Similarly, fast-merging BNS, potentially originating from dynamical interactions in dense stellar environments such as globular clusters or galactic nuclei [46, 47], may exhibit distinct ejecta properties and shorter merger timescales compared to field BNSs [48]. Both channels have been speculated as potential candidates to explain the short-fall in the observed abundance evolution, particularly under the assumption that they are either prompt and/or more efficient ejectors [23, 49–54]. Our goal here is to do a rigorous data-supported assessment of the viability of these two channels to fill in the missing components in the origin of heavy elements in the Milky Way.

Using a likelihood-based inference framework proposed in [32], we quantify the extent to which the NSBH and fast-merging BNS channels can contribute to the observed evolution of [Eu/Fe] versus [Fe/H]. In doing so, we also examine whether the required conditions are astrophysically plausible given current constraints on merger rates, delay times, and ejecta properties.

The remainder of this paper is organized as follows. In Methods, we outline the chemical evolution model and describe our inference framework. In Results, we discuss results for the three scenarios: fast-merging BNS assumed to be GW-detectable, fast-merging BNS assumed to be GW-undetectable, and NSBH as a secondary channel. Finally, we summarize our findings and discuss their implications for the origin of r -process elements in the Milky Way.

II. METHODS

A. Chemical Evolution Framework with Multiple r -process Channels

Our chemical evolution model, incorporating multiple candidate r -process enrichment channels, builds directly upon the one-zone prescription employed in [32], which

in turn follows the approach of [35]. In this framework, the Milky Way is treated as a single, well-mixed reservoir of interstellar medium (ISM). The model evolves the abundances of heavy elements over cosmic time by integrating nucleosynthesis yields from astrophysical events convolved with their respective rate over time. If the astrophysical events were delayed relative to the SFR, we adopt a delay-time model, which is a power law distribution with minimum delay time (t_{\min}) and slope (α) as parameters (e.g. Eq. 2 in [37]). For a given SFR, delay-time model, and event yields, the model tracks the enrichment history in both α and iron-peak elements, as well as r -process elements such as Eu.

Key enrichment channels in the baseline model include core-collapse supernovae (CCSNe) and Type Ia supernovae (SNe Ia), mainly contributing to α and iron enrichment, respectively. The r -process enrichment is primarily attributed to delayed BNS mergers, but the model is flexible enough to include additional candidate channels such as fast-merging BNS systems and NSBH mergers, as we explore in this work. Each r -process channel is described by its local event rate, the average event yield, a delay-time model or one that directly follows the SFR without additional parameters needed.

The evolution of the ISM, in addition to all the contributions from various channels, is also governed by a mass-loss term due to star formation and Galactic outflows, which scales with the SFR and which was calibrated in previous work [17]. For CCSNe and SNe Ia, we follow the same rates and yields for iron production as in [35]. Thus, the only free parameters in our model are for the r -process sources. Given an arbitrary choice of parameters describing each r -process channel, the model produces predictions for the time evolution of abundance ratios such as [Fe/H] and [Eu/Fe]. It is this [Eu/Fe] versus [Fe/H] abundance evolution track that we compare with the observed stellar abundance distributions to constrain possible r -process enrichment channels.

B. Likelihood Model and Bayesian Inference Framework

The stellar abundance data of the disk stars we use are from Ref. [55]. To quantify the agreement between model predictions and stellar abundance data, we adopt the likelihood formalism introduced in Ref. [32]. Each observed disk star is represented as a 2D Gaussian in ([Fe/H], [Eu/Fe]) space, centered on the measured values with widths set by observational uncertainties [55]. We use only disk stars, as the one-zone chemical evolution model assumes a well-mixed ISM—an assumption more appropriate for the Galactic disk than for the halo. Halo stars, which formed earlier in more chemically inhomogeneous environments [56–59], are therefore excluded.

The chemical evolution model described in previous subsection generates a time-ordered track in the same abundance space, and the likelihood for each star is com-

puted by integrating its Gaussian distribution over the model track. The total likelihood is the product over all stars, evaluated numerically. We use this likelihood for Bayesian inference on the parameters governing each r -process channel, including the local event rate, yield, and, where applicable, the minimum delay time (t_{\min}) and delay-time distribution power-law index (α). Priors on the local merger rates as a function of binary mass and event yield are formulated from GW-inferred population properties of GWTC-4.0 catalog [60], pulsar observations [40], and semi-analytical fits to numerical simulations [41], while priors on the delay-time distribution parameters are obtained from sGRB constraints [37]. We use the **Dynesty** sampler via the **Bilby** inference framework to sample from the likelihood surface [61, 62].

III. RESULTS

A. Current GW searches can detect fast-merging BNSs

We first examine whether a population of fast-merging BNS can account for the missing r -process enrichment. In some extreme scenarios, the fast-merging BNSs may be difficult to search with current GW detection pipelines. For example, BNSs with high eccentricities may be missed. These systems are expected to form in dense stellar environments such as globular clusters or nuclear star clusters [63–65], where close interactions can lead to highly eccentric binaries. The resulting rapid inspirals may exhibit significantly fewer in-band GW cycles, producing waveforms that are poorly matched to standard quasi-circular templates [66]. This reduces their detection probability and may lead to systematic biases in parameter estimation [67].

In this subsection, we discuss the scenario that fast-merging systems are detectable with the same efficiency as delayed BNS mergers. We will discuss the scenario that the fast-merging population is missed from current observations in the next subsection. While these are two extreme scenarios, the reality is likely to be in between the results we find from these two scenarios.

If the fast-merging population is detectable, current GW-inferred BNS merger rates should encompass both delayed and fast-merging systems. The total r -process contribution from BNS mergers is then a mixture of both components. We parameterize the fraction f_{fast} of total BNS mergers that are fast-merging as

$$\begin{aligned} R_{\text{fast}} &= f_{\text{fast}} \cdot R_{\text{BNS}}, \text{ and} \\ R_{\text{delayed}} &= (1 - f_{\text{fast}}) \cdot R_{\text{BNS}}, \end{aligned}$$

where R_{BNS} is the total BNS rate, R_{fast} is the fast-merging BNS rate, and R_{delayed} is the delayed BNS rate. We assume delayed BNS mergers follow an sGRB-informed delay-time distribution [37], while fast-merging BNSs are assumed to be SFR-tracking (i.e., zero delay

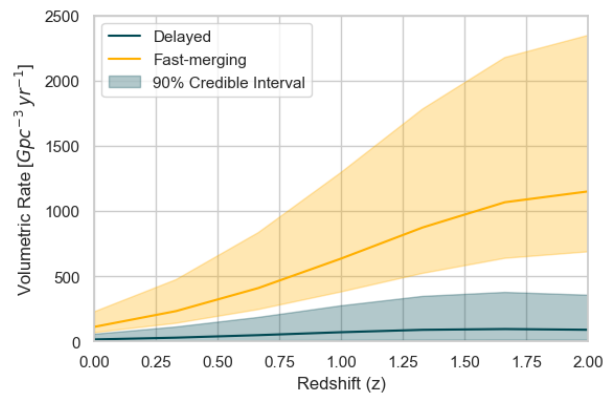


FIG. 1. Comoving BNS merger-rate density as a function of redshift for the delayed and fast-merging BNS channels, required if they were solely to explain the [Eu/Fe] versus [Fe/H] abundance trends observed from Milky Way’s disk stars. Solid curves are posterior medians; shaded regions show central 90% credible intervals. Here, we assume the fast-merging systems are detectable by current gravitational-wave searches and have no delay relative to SFR. The figure shows that the fast-merging BNSs have to dominate the BNS rates across the Milky Way history in order to explain the observed abundance trends.

time). Because of the differing evolution of rates for the two channels, the above rates and f_{fast} are functions of redshift. We then infer f_{fast} under this dual-BNS population scenario.

We assume that all BNS populations share the same neutron star EOS and model of event yield [32, 41].

Our inference shows that reproducing the observed [Eu/Fe] trend in this scenario requires an exceptionally high fast-merging fraction. The posterior for f_{fast} in the local Universe ($z = 0$) peaks near unity, with more than 71% of BNS mergers inferred to be fast-merging (90% confidence lower limit). This fraction goes up to $> 74\%$ at $z = 1$ and $> 80\%$ at $z = 2$, as a SFR-tracking channel is expected to contribute more frequently in the early Universe compared to delayed sources. In Figure 1, we show the corresponding volumetric rate as a function of redshift. In particular, the local ($z = 0$) volumetric rate of the fast-merging BNS is $110^{+115}_{-44} \text{ Gpc}^{-3} \text{ yr}^{-1}$ while the delayed BNS rate remains at a lower level of $14^{+40}_{-13} \text{ Gpc}^{-3} \text{ yr}^{-1}$, where the error bars correspond to 90% credible levels (The reader may refer to Appendix and Fig. 4 for the posteriors of all inferred parameters.). Since this analysis assumes that GW searches are sensitive to both channels, the sum of the two channels is limited by the GW-inferred local BNS rate ($z = 0$). It will not be the case for our analysis in the next subsection.

These findings suggest that, even with zero delay time, the fast-merging BNSs have to show a near-total dominance in the entire BNS population in order to account for the r -process abundance evolution in the Milky Way—specifically the negative slope in [Eu/Fe] versus

[Fe/H] for the disk stars. This scenario poses a strong tension with the current understanding of fast-merging BNS populations [34, 68, 69], and hence challenges the idea that they are the primary explanation for Galactic r -process enrichment.

B. Current GW searches miss fast-merging BNSs

In this scenario, we consider the possibility that fast-merging BNSs constitute a distinct subpopulation that is *not* captured by current GW searches. We note that although eccentric systems are good examples, our study applies to *any* scenario in which fast-merging BNSs are missed.

To model this population, we assume that delayed BNS mergers follow the standard GW-inferred rate and sGRB-informed delay-time distribution [37], as in the previous subsection. We then introduce an additional r -process channel composed of GW-undetectable fast-merging BNS systems. This additional population is assumed to track the SFR.

The contribution from this channel is parameterized using a multiplicative enhancement factor X_{fast} , such that the total rate from undetectable fast-merging BNS mergers is:

$$R_{\text{fast}} = X_{\text{fast}} \cdot R_{\text{BNS}},$$

where R_{BNS} is the rate of *delayed* BNS mergers. The local ($z = 0$) value of R_{BNS} is inferred from GW observations. Again, the rates and X_{fast} are functions of redshift.

Our analysis finds that, in order to explain the observed [Eu/Fe] versus [Fe/H] trend (negative slope for disk stars, as mentioned before) with only delayed and undetected fast-merging BNSs, the multiplicative factor X_{fast} is estimated to be $9.0^{+10.0}_{-6.0}$ in the local Universe (90% confidence lower limit), while it further rises up to $11.0^{+11.0}_{-8.0}$ at $z = 1$ and $15.0^{+18.0}_{-11.0}$ at $z = 2$. Equivalently, the fast-merging BNS rate would be $R_{\text{fast}} = 391.0^{+472.0}_{-230.0} \text{ Gpc}^{-3} \text{ yr}^{-1}$ in the local Universe (Figure 2, 90% confidence lower limit), and R_{fast} goes up to $2251.0^{+2716.0}_{-1327.0} \text{ Gpc}^{-3} \text{ yr}^{-1}$ at $z = 1$ and $4078.0^{+4919.0}_{-2404.0} \text{ Gpc}^{-3} \text{ yr}^{-1}$ at $z = 2$. This implies that the Milky Way would require roughly 9 times (median value) as many fast-merging BNSs as delayed ones; this outcome again challenges the current understanding of the delayed and fast-merging BNS rates [34, 68, 69] (The reader may refer to Appendix and Fig. 5 for the posteriors of all inferred parameters.).

From the results in the previous and this subsection, we conclude that fast-merging BNSs, even with SFR-tracking rates, are difficult to resolve the r -process enrichment discrepancy without invoking an extremely high occurrence rate relative to the delayed systems.

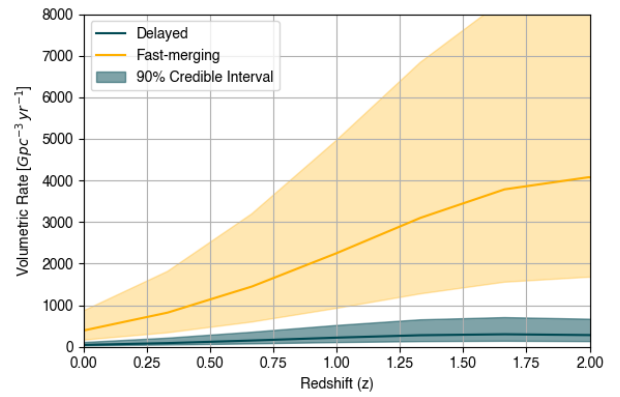


FIG. 2. Same as Fig. 1 but under the assumption that the gravitational-wave searches are not sensitive to fast-merging BNS events. The figure shows that a gravitational-wave undetectable fast-merging BNS population can explain the observed r -process abundance trends only if their merger rate significantly exceeds that of the delayed population across the Milky Way history.

C. NSBH Mergers as a Secondary Channel

In this subsection, we assess whether the combined contributions of BNS and NSBH mergers can explain the observed Eu enrichment in the Milky Way. To that end, we construct a joint four-dimensional distribution over the local merger rates and yields of BNS and NSBH systems, following the methodology of [70] and using the fitting formulae from [41] for the yield with uncertainties. We use this distribution as priors for our chemical evolution modeling.

As mentioned earlier, the BNS delay-time distribution parameters (α , t_{min}) are sampled from sGRB-informed constraints [37]. The delay time for NSBH mergers is uncertain. It could follow the sGRB delay time, or have a completely different delay-time distribution. If NSBH mergers promptly merge with no delay relative to the SFR, it would contribute most to rectify the difference between the delayed BNS-only evolution track and the [Eu/Fe] versus [Fe/H] observations, as motivated by [32]. We start with this assumption.

We find that even under optimistic delay-time distribution assumptions to maximize the contribution from NSBH, the combined BNS and NSBH channels fail to reproduce the observed [Eu/Fe] trends.

To allow for residual enrichment not captured by BNS and NSBH channels, we then add a third, phenomenological channel whose rate also tracks the SFR. Its contribution is parameterized as a fraction of the total r -process enrichment, as its rate and yield are unknown. This component captures any dominant but currently unidentified source of early-time Eu production.

Figure 3 shows the inferred (rate \times yield) fraction integrated over cosmic history until present day, from the BNS (blue), NSBH (orange), and third (green) channels.

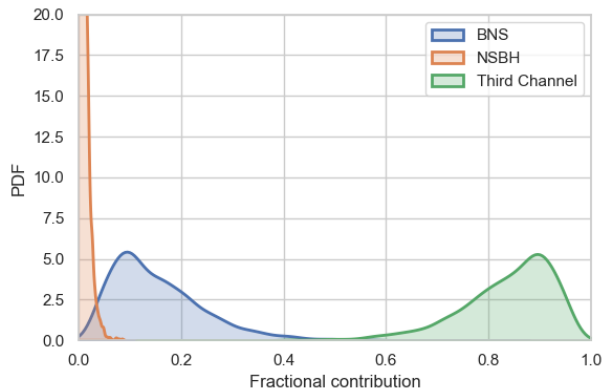


FIG. 3. Posterior distributions for the BNS (blue), NSBH (orange), and third-channel (green) r -process contributions. We show the fractional contribution from each channel integrated over cosmic history, inferred simultaneously to best fit the observed abundance data from Milky Way disk stars.

The BNS contribution is consistent with the findings of [32], while the NSBH contribution remains marginal. In contrast, the third, phenomenological SFR-tracking channel dominates the posterior. Quantitatively, at 90% confidence, more than 70% of the contribution must be from the unknown third channel while the combined contribution from BNS and NSBH is limited to below 30% (The reader may refer to Appendix and Fig. 6 for the posteriors of all inferred parameters.). These results underscore that BNS and NSBH mergers alone cannot account for the observed $[\text{Eu}/\text{Fe}]$ versus $[\text{Fe}/\text{H}]$ trend, and that a substantial additional source of r -process elements is required.

IV. DISCUSSION AND CONCLUSION

We have investigated whether fast-merging BNSs or NSBH mergers can resolve the r -process enrichment discrepancy identified previously [16, 18, 21, 32, 35, 71], where BNS mergers fail to reproduce the observed Eu trends—the negative slope in $[\text{Eu}/\text{Fe}]$ versus $[\text{Fe}/\text{H}]$ —in the Milky Way disk. Across all three scenarios explored—GW-detectable fast-merging BNSs, GW-undetectable fast-merging BNSs, and NSBH mergers—we find that these channels are unlikely to serve as the dominant source of r -process enrichment.

Although the sGRB host observations used to infer the delay-time distribution [37] may suffer from selection biases that favor nearby events, potentially missing fast-merging systems occurring at higher redshifts, our analysis shows that the fast-merging population must be significantly larger than the delayed population—even in the local Universe. This result raises several major challenges for both theories and observations:

1. What is the coherent theoretical framework that explains why fast-merging BNSs form significantly

more efficiently than delayed systems across the Milky Way history?

2. Even if high-redshift hosts of sGRBs are missed, why do nearby sGRBs predominantly exhibit long delay times, in apparent contradiction with the presence of a large fast-merging population?
3. If instead fast-merging BNSs do not produce observable sGRBs, but do synthesize substantial quantities of r -process elements (possibly accompanied by significant amount of kilonovae), what distinguishes their counterpart production mechanisms from those of delayed BNS mergers?
4. If a large number of fast-merging BNSs exist that are not detectable in GWs, why have current GW search pipelines—both modeled and unmodeled [72]—not identified nearby events with high signal-to-noise ratios, especially given that some of these should be detectable even if existing waveform models are suboptimal?

We emphasize that, although the fast-merging BNS and NSBH populations may not precisely follow the assumed star formation rate, may have different yields from those estimated with semi-analytical fit, may have mass distributions that differ from those inferred from GW observations, and/or may not adhere to the assumed r -process abundance pattern—all of which could affect their event rates or Eu yields—our analysis still indicates that an exceptionally large contribution from these channels is required across cosmic history (see the required fractions and volumetric rates in the *Results* section). This poses a substantial challenge to constructing a consistent theoretical framework. For instance, to reduce the event rates of fast-merging BNSs or NSBHs to a level comparable to that of delayed BNSs, their Eu yield would need to be increased by a factor of $\gtrsim 5$. This requires a scenario that boosts their yields by $\gtrsim 5$ times *without increasing the delayed BNS yield*. Similarly, even if the early-Universe evolution of these populations differs from our assumptions, they would still need to occur much more frequently than delayed BNSs to reproduce the observed trends in stellar metallicity.

Our findings not only reinforce the conclusions of [32], but also pose substantial challenges to two leading candidates—fast-merging BNS and NSBH systems—as dominant r -process enrichment channels. These results help narrow down the viable r -process sources in the Milky Way and strongly suggest that non-merger pathways are needed to explain the observed abundances.

ACKNOWLEDGMENTS

The authors would like to thank Floor Broekgaarden, Wen-fai Fong, Francois Foucart, Erika Holmbeck, and Alexander Ji for very helpful discussions. M.S.

is supported by the Weinberg Institute for Theoretical Physics at the University of Texas at Austin. H.-Y.C. is supported by the National Science Foundation under Grant PHY-2308752 and Department of Energy Grant DE-SC0025296. The authors are grateful for computational resources provided by the LIGO Laboratory and supported by National Science Foundation Grants PHY-0757058 and PHY-0823459. This material is based upon work supported by NSF’s LIGO Laboratory which is a major facility fully funded by the National Science Foundation.

Appendix A: Additional details for all three cases

In this appendix, we present additional plots that shed light on further details of each of the three analyses discussed in the main text. Figure 4 shows corner plots of the posterior distributions for all model parameters: the total BNS rate R_{BNS} (including both delayed and fast-merging channels); the ejecta mass m_{ej} (assumed common to both channels); the delay-time parameters α and t_{min} of the delayed BNS channel; and the fraction f_{fast} , which specifies the portion of R_{BNS} assigned to the fast-merging channel required to reproduce the

observed abundance trends of Milky Way disk stars [55]. The large panel in the upper right shows the 90% credible regions (orange) in the $[\text{Eu}/\text{Fe}]$ – $[\text{Fe}/\text{H}]$ plane implied by the posterior samples; observed abundances from [55] are overplotted as blue points.

Fig. 5 presents the similar details for the analysis discussed in Fig. 2, in which R_{BNS} refers exclusively to the *delayed* BNS channel. The ejecta mass m_{ej} is again taken to be common, and the fast component is encoded via a multiplicative factor X_{fast} such that $R_{\text{fast}} = X_{\text{fast}} R_{\text{BNS}}$.

Finally, Fig. 6 summarizes the analysis in which we include both BNS and NSBH contributions with an agnostic third channel to capture any residual enrichment not accounted for by them. The sampled parameters are the rate times mass ejecta products $\mathcal{Y}_{\text{BNS}} \equiv R_{\text{BNS}} m_{\text{ej}}^{\text{BNS}}$ and $\mathcal{Y}_{\text{NSBH}} \equiv R_{\text{NSBH}} m_{\text{ej}}^{\text{NSBH}}$, the BNS channel delay-time parameters (α, t_{min}) , and a fractional contribution parameter f_3 that encodes the third channel’s share of the total mass-injection rate (we take $\mathcal{Y}_3 = f_3 \mathcal{Y}_{\text{tot}}$ with $\mathcal{Y}_{\text{tot}} = \mathcal{Y}_{\text{BNS}} + \mathcal{Y}_{\text{NSBH}} + \mathcal{Y}_3$). The large panel at upper right again shows the posterior-predicted credible regions in the $[\text{Eu}/\text{Fe}]$ – $[\text{Fe}/\text{H}]$ plane with the same observational sample overplotted.

-
- [1] E. M. Burbidge, G. R. Burbidge, W. A. Fowler, and F. Hoyle, *Rev. Mod. Phys.* **29**, 547 (1957).
 - [2] A. G. W. Cameron, *PASP* **69**, 201 (1957).
 - [3] J. M. Lattimer and D. N. Schramm, *ApJ* **192**, L145 (1974).
 - [4] D. Eichler, M. Livio, T. Piran, and D. N. Schramm, *Nature* **340**, 126 (1989).
 - [5] C. Freiburghaus, S. Rosswog, and F. K. Thielemann, *ApJ* **525**, L121 (1999).
 - [6] B. P. e. a. L. S. C. Abbott and V. Collaboration), *Phys. Rev. Lett.* **119**, 161101 (2017).
 - [7] B. P. Abbott *et al.* (LIGO Scientific, Virgo, Fermi GBM, INTEGRAL, IceCube, AstroSat Cadmium Zinc Telluride Imager Team, IPN, Insight-Hxmt, ANTARES, Swift, AGILE Team, 1M2H Team, Dark Energy Camera GW-EM, DES, DLT40, GRAWITA, Fermi-LAT, ATCA, ASKAP, Las Cumbres Observatory Group, OzGrav, DWF (Deeper Wider Faster Program), AST3, CAAS-TRO, VINROUGE, MASTER, J-GEM, GROWTH, JAGWAR, CaltechNRAO, TTU-NRAO, NuSTAR, Pan-STARRS, MAXI Team, TZAC Consortium, KU, Nordic Optical Telescope, ePESSTO, GROND, Texas Tech University, SALT Group, TOROS, BOOTES, MWA, CALET, IKI-GW Follow-up, H.E.S.S., LOFAR, LWA, HAWC, Pierre Auger, ALMA, Euro VLBI Team, Pi of Sky, Chandra Team at McGill University, DFN, ATLAS Telescopes, High Time Resolution Universe Survey, RIMAS, RATIR, SKA South Africa/MeerKAT), *Astrophys. J. Lett.* **848**, L12 (2017), [arXiv:1710.05833 \[astro-ph.HE\]](#).
 - [8] D. Kasen, B. D. Metzger, J. Barnes, E. Quataert, and E. Ramirez-Ruiz, *Nature* **551**, 80 (2017).
 - [9] S. Rosswog, *ApJ* **634**, 1202 (2005).
 - [10] K. Kyutoku, K. Ioka, H. Okawa, M. Shibata, and K. Taniguchi, *Phys. Rev. D* **92**, 044028 (2015).
 - [11] C. e. a. Winteler, *ApJ* **750**, L22 (2012).
 - [12] N. Nishimura, T. Takiwaki, and F.-K. Thielemann, *ApJ* **810**, 109 (2015).
 - [13] D. M. Siegel, J. Barnes, and B. D. Metzger, *Nature* **569**, 241 (2019).
 - [14] J. Cehula, T. A. Thompson, and B. D. Metzger, *Mon. Not. Roy. Astron. Soc.* **528**, 5323 (2024), [arXiv:2311.05681 \[astro-ph.HE\]](#).
 - [15] A. Patel, B. D. Metzger, J. Cehula, E. Burns, J. A. Goldberg, and T. A. Thompson, *Astrophys. J. Lett.* **984**, L29 (2025), [arXiv:2501.09181 \[astro-ph.HE\]](#).
 - [16] B. e. a. Côté, *ApJ* **875**, 106 (2019).
 - [17] K. Hotokezaka, P. Beniamini, and T. Piran, *Int. J. Mod. Phys. D* **27**, 1842005 (2018), [arXiv:1801.01141 \[astro-ph.HE\]](#).
 - [18] F. van de Voort, E. Quataert, P. F. Hopkins, D. Kereš, and C.-A. Faucher-Giguère, *Monthly Notices of the Royal Astronomical Society* **447**, 140 (2015), [arXiv:1407.7039 \[astro-ph.GA\]](#).
 - [19] G. Cescutti, D. Romano, F. Matteucci, C. Chiappini, and R. Hirschi, *Astronomy & Astrophysics* **577**, A139 (2015), [arXiv:1503.02954 \[astro-ph.GA\]](#).
 - [20] F. van de Voort, R. Pakmor, R. Bieri, and R. J. J. Grand, *Mon. Not. Roy. Astron. Soc.* **512**, 5258 (2022), [arXiv:2110.11963 \[astro-ph.GA\]](#).
 - [21] C. Kobayashi *et al.*, *Astrophys. J. Lett.* **943**, L12 (2023), [arXiv:2211.04964 \[astro-ph.HE\]](#).
 - [22] A. N. Kolborg, E. Ramirez-Ruiz, D. Martizzi, P. Macias, and M. Soares-Furtado, *Astrophys. J.* **949**, 100 (2023),

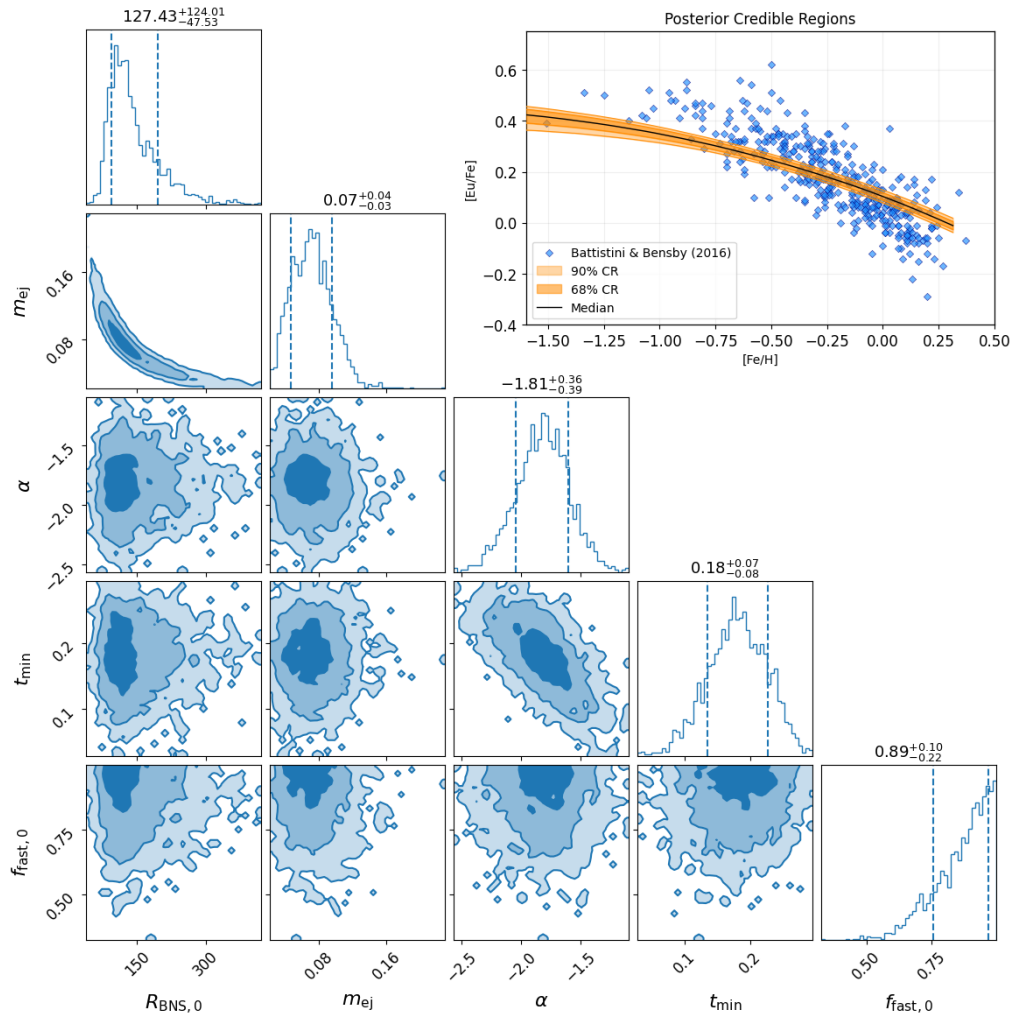


FIG. 4. **Current GW searches can detect fast-merging BNSs.** Diagonal panels show marginalized posteriors (medians and 68% credible intervals); off-diagonal panels show joint posteriors (filled credible regions). Parameters are the total BNS rate R_{BNS} ($\text{Gpc}^{-3} \text{yr}^{-1}$), ejecta mass m_{ej} (M_{\odot}), delayed-channel delay-time parameters α and t_{min} , and the fast-merging fraction f_{fast} . The subscript ‘0’ in the parameter labels indicate that all these quantities are evaluated in the local universe ($z = 0$). The large panel at upper right displays the posterior-predicted credible regions (orange) in $[\text{Eu}/\text{Fe}]$ versus $[\text{Fe}/\text{H}]$, with Milky Way disk measurements from [55] shown as blue points.

- arXiv:2304.01144 [astro-ph.GA].
- [23] M. Bonetti, A. Perego, M. Dotti, and G. Cescutti, *Mon. Not. Roy. Astron. Soc.* **490**, 296 (2019), arXiv:1905.12016 [astro-ph.HE].
- [24] M. Zevin, K. Kremer, D. M. Siegel, S. Coughlin, B. T. H. Tsang, C. P. L. Berry, and V. Kalogera, (2019), 10.3847/1538-4357/ab498b, arXiv:1906.11299 [astro-ph.HE].
- [25] Á. Skúladóttir, C. J. Hansen, S. Salvadori, and A. Choplin, *Astronomy & Astrophysics* **631**, A171 (2019), arXiv:1908.10729 [astro-ph.GA].
- [26] R. P. Naidu *et al.*, *Astrophys. J. Lett.* **926**, L36 (2022), arXiv:2110.14652 [astro-ph.GA].
- [27] J. D. Simon, T. M. Brown, B. Mutlu-Pakdil, A. P. Ji, A. Drlica-Wagner, R. J. Avila, C. E. Martínez-Vázquez, T. S. Li, E. Balbinot, K. Bechtol, A. Frebel, M. Geha, T. T. Hansen, D. J. James, A. B. Pace, M. Agüena, O. Alves, F. Andrade-Oliveira, J. Annis, D. Bacon, E. Bertin, D. Brooks, D. L. Burke, A. Carnero Rosell, M. Carrasco Kind, J. Carretero, M. Costanzi, L. N. da Costa, J. De Vicente, S. Desai, P. Doel, S. Everett, I. Ferrero, J. Frieman, J. García-Bellido, M. Gatti, D. W. Gerdes, D. Gruen, R. A. Gruendl, J. Gschwend, G. Gutierrez, S. R. Hinton, D. L. Hollowood, K. Honscheid, K. Kuehn, N. Kuropatkin, J. L. Marshall, J. Mena-Fernández, R. Miquel, A. Palmese, F. Paz-Chinchón, M. E. S. Pereira, A. Pieres, A. A. Plazas Malagón, M. Raveri, M. Rodríguez-Monroy, E. Sanchez, B. Santiago, V. Scarpine, I. Sevilla-Noarbe, M. Smith, E. Suchyta, M. E. C. Swanson, G. Tarle, C. To, M. Vincenzi, N. Weaverdyck, and R. D. Wilkinson, *Astrophys. J.* **944**, 43 (2023), arXiv:2212.00810 [astro-ph.GA].
- [28] E. N. Kirby, A. P. Ji, and M. Kovalev, *Astrophys. J.* **958**, 45 (2023), arXiv:2308.10980 [astro-ph.SR].
- [29] C. Sneden, J. J. Cowan, and R. Gallino, *Annual Review*

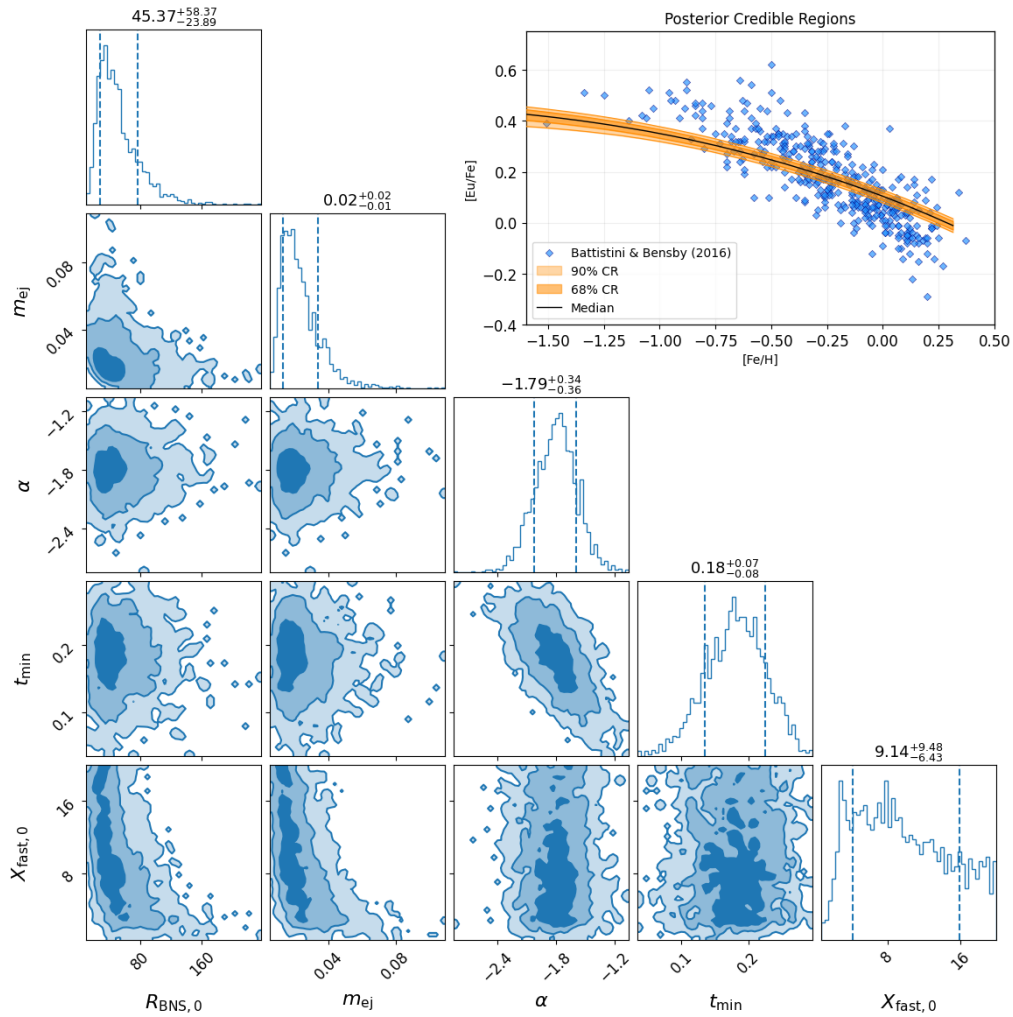


FIG. 5. **Current GW searches miss fast-merging BNSs.** Diagonal panels show marginalized posteriors (medians and 68% credible intervals); off-diagonal panels show joint posteriors (filled credible regions). Parameters are the delayed-channel BNS merger rate R_{BNS} ($\text{Gpc}^{-3} \text{yr}^{-1}$) (here referring to the *delayed* component only), the common ejecta mass m_{ej} (M_{\odot}), the delayed-channel delay-time parameters α and t_{min} , and the scaling factor X_{fast} that sets the fast-merging rate as $R_{\text{fast}} = X_{\text{fast}} R_{\text{BNS}}$. The subscript ‘0’ in the parameter labels indicate that all these quantities are evaluated in the local universe ($z = 0$). The large panel at upper right displays the posterior-predicted credible regions (orange) in $[\text{Eu}/\text{Fe}]$ versus $[\text{Fe}/\text{H}]$, with Milky Way disk measurements from [55] shown as blue points.

- of Astronomy and Astrophysics **46**, 241 (2008).
- [30] A. Frebel, *Astronomische Nachrichten* **331**, 474 (2010), [arXiv:1006.2419 \[astro-ph.GA\]](#).
 - [31] M. Cain, A. Frebel, A. P. Ji, V. M. Placco, R. Ezzeddine, I. U. Roederer, K. Hattori, T. C. Beers, J. Meléndez, T. T. Hansen, and C. M. Sakari, *Astrophys. J.* **898**, 40 (2020), [arXiv:2006.08080 \[astro-ph.SR\]](#).
 - [32] H.-Y. Chen, P. Landry, J. S. Read, and D. M. Siegel, *Astrophys. J.* **985**, 154 (2025), [arXiv:2402.03696 \[astro-ph.HE\]](#).
 - [33] P. C. Peters, *Phys. Rev.* **136**, B1224 (1964).
 - [34] P. Beniamini and T. Piran, *Mon. Not. Roy. Astron. Soc.* **487**, 4847 (2019), [arXiv:1903.11614 \[astro-ph.HE\]](#).
 - [35] D. M. Siegel, J. Barnes, and B. D. Metzger, *Nature* **569**, 241 (2019), [arXiv:1810.00098 \[astro-ph.HE\]](#).
 - [36] P. Madau and T. Fragos, *Astrophys. J.* **840**, 39 (2017), [arXiv:1606.07887 \[astro-ph.GA\]](#).
 - [37] M. Zevin, A. E. Nugent, S. Adhikari, W.-f. Fong, D. E. Holz, and L. Z. Kelley, *Astrophys. J. Lett.* **940**, L18 (2022), [arXiv:2206.02814 \[astro-ph.HE\]](#).
 - [38] R. Abbott *et al.* (KAGRA, VIRGO, LIGO Scientific), *Phys. Rev. X* **13**, 041039 (2023), [arXiv:2111.03606 \[gr-qc\]](#).
 - [39] R. Abbott *et al.* (KAGRA, VIRGO, LIGO Scientific), *Phys. Rev. X* **13**, 011048 (2023), [arXiv:2111.03634 \[astro-ph.HE\]](#).
 - [40] I. Legred, K. Chatziioannou, R. Essick, S. Han, and P. Landry, *Phys. Rev. D* **104**, 063003 (2021), [arXiv:2106.05313 \[astro-ph.HE\]](#).
 - [41] C. J. Krüger and F. Foucart, *Phys. Rev. D* **101**, 103002 (2020), [arXiv:2002.07728 \[astro-ph.HE\]](#).
 - [42] D. Wanderman and T. Piran, *Mon. Not. Roy. Astron. Soc.* **448**, 3026 (2015), [arXiv:1405.5878 \[astro-ph.HE\]](#).
 - [43] G. Ghirlanda *et al.*, *Astron. Astrophys.* **594**, A84 (2016),

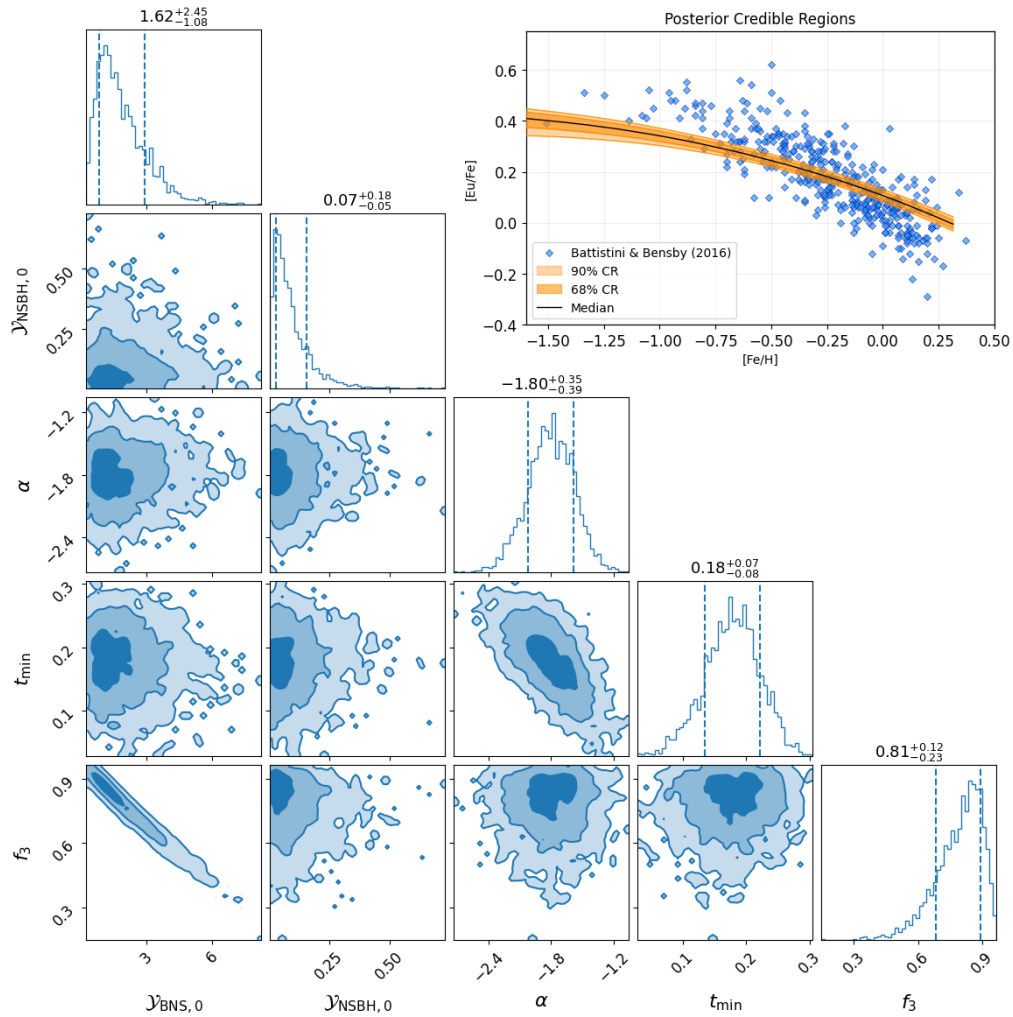


FIG. 6. **NSBH Mergers as a Secondary Channel.** Diagonal panels show marginalized posteriors (medians and 68% credible intervals); off-diagonal panels show joint posteriors (filled credible regions). Parameters are the rate times mass ejecta products $\mathcal{Y}_{\text{BNS}} = R_{\text{BNS}} m_{\text{ej}}^{\text{BNS}}$ and $\mathcal{Y}_{\text{NSBH}} = R_{\text{NSBH}} m_{\text{ej}}^{\text{NSBH}}$ ($\text{M}_{\odot} \text{Gpc}^{-3} \text{yr}^{-1}$), the BNS delay-time parameters (α, t_{min}), and the fractional third-channel contribution f_3 defined via $\mathcal{Y}_3 = f_3 \mathcal{Y}_{\text{tot}}$. The subscript ‘0’ in the parameter labels indicate that all these quantities are evaluated in the local universe ($z = 0$). The large panel at upper right displays the posterior-predicted credible regions (orange) in $[\text{Eu}/\text{Fe}]$ versus $[\text{Fe}/\text{H}]$, with Milky Way disk measurements from [55] shown as blue points.

- arXiv:1607.07875 [astro-ph.HE].
- [44] F. Foucart, T. Hinderer, and S. Nissanke, *Phys. Rev. D* **98**, 081501 (2018), arXiv:1807.00011 [astro-ph.HE].
 - [45] M. Mapelli, N. Giacobbo, M. Toffano, E. Ripamonti, A. Bressan, M. Spera, and M. Branchesi, *Mon. Not. Roy. Astron. Soc.* **481**, 5324 (2018), arXiv:1809.03521 [astro-ph.HE].
 - [46] J. Samsing *et al.*, *Phys. Rev. D* **97**, 103014 (2018).
 - [47] C. L. Rodriguez *et al.*, *Phys. Rev. D* **98**, 123005 (2018).
 - [48] A. Vigna-Gómez *et al.*, *Mon. Not. Roy. Astron. Soc.* **481**, 4009 (2018), arXiv:1805.07974 [astro-ph.SR].
 - [49] M. Safarzadeh, E. Ramirez-Ruiz, J. J. Andrews, T. Fragos, P. Macias, and E. Scannapieco, *Astrophys. J.* **872**, 105 (2019), arXiv:1810.04176 [astro-ph.HE].
 - [50] J. J. Andrews and A. Zezas, *Mon. Not. Roy. Astron. Soc.* **486**, 3213 (2019), arXiv:1904.06137 [astro-ph.HE].
 - [51] P. Beniamini and T. Piran, *Astrophys. J.* **966**, 17 (2024), arXiv:2312.02269 [astro-ph.HE].
 - [52] A. E. Nugent, W.-f. Fong, C. Castrejon, J. Leja, M. Zevin, and A. P. Ji, *Astrophys. J.* **962**, 5 (2024), arXiv:2310.12202 [astro-ph.GA].
 - [53] E. M. Holmbeck and J. J. Andrews, *Astrophys. J.* **963**, 110 (2024), arXiv:2310.03847 [astro-ph.HE].
 - [54] D. Maoz and E. Nakar, *Astrophys. J.* **982**, 179 (2025), arXiv:2406.08630 [astro-ph.HE].
 - [55] C. Battistini and T. Bensby, *Astronomy & Astrophysics* **586**, A49 (2016), arXiv:1511.00966 [astro-ph.SR].
 - [56] A. J. Deason and V. Belokurov, *New Astronomy Reviews* **99**, 101706 (2024).
 - [57] J. T. Mackereth, R. P. Schiavon, J. Pfeffer, C. R. Hayes, J. Bovy, B. Anguiano, C. Allende Prieto, S. Hasegawa, J. Holtzman, J. A. Johnson, S. R. Majewski, R. O’Connell, M. Shetrone, P. B. Tissera, and J. G. Fernández-Trincado, *Monthly Notices of the Royal Astronomical Society* **482**, 3426 (2019), arXiv:1808.00968 [astro-ph.GA].

- [58] S. Khoperskov, I. Minchev, N. Libeskind, M. Haywood, P. Di Matteo, V. Belokurov, M. Steinmetz, F. A. Gomez, R. J. J. Grand, Y. Hoffman, A. Knebe, J. G. Sorce, M. Spaare, E. Tempel, and M. Vogelsberger, *Astronomy & Astrophysics* **677**, A89 (2023), [arXiv:2206.04521 \[astro-ph.GA\]](#).
- [59] D. de Brito Silva, P. Jofré, C. Worley, K. Hawkins, and P. Das, *Astronomy & Astrophysics* **690**, A120 (2024), [arXiv:2407.18851 \[astro-ph.GA\]](#).
- [60] The LIGO Scientific Collaboration, the Virgo Collaboration, the KAGRA Collaboration (LIGO Scientific, VIRGO, KAGRA), (2025), [arXiv:2508.18083 \[astro-ph.HE\]](#).
- [61] J. S. Speagle, *Monthly Notices of the Royal Astronomical Society* **493**, 3132 (2020).
- [62] G. Ashton, M. Huebner, P. D. Lasky, *et al.*, *Astrophys. J. Suppl.* **241**, 27 (2019), [arXiv:1811.02042 \[astro-ph.IM\]](#).
- [63] J. Samsing, M. MacLeod, and E. Ramirez-Ruiz, *Astrophys. J.* **784**, 71 (2014), [arXiv:1308.2964 \[astro-ph.HE\]](#).
- [64] C. L. Rodriguez, P. Amaro-Seoane, S. Chatterjee, and F. A. Rasio, *Phys. Rev. Lett.* **120**, 151101 (2018), [arXiv:1712.04937 \[astro-ph.HE\]](#).
- [65] G. Fragione, E. Grishin, N. W. C. Leigh, H. B. Perets, and R. Perna, *Mon. Not. Roy. Astron. Soc.* **488**, 47 (2019), [arXiv:1811.10627 \[astro-ph.GA\]](#).
- [66] S. V. Chaurasia, T. Dietrich, N. K. Johnson-McDaniel, M. Ujevic, W. Tichy, and B. Brügmann, *Phys. Rev. D* **98**, 104005 (2018), [arXiv:1807.06857 \[gr-qc\]](#).
- [67] G. Huez, S. Bernuzzi, M. Breschi, and R. Gamba, (2025), [arXiv:2504.18622 \[gr-qc\]](#).
- [68] K. Belczynski *et al.*, (2018), [arXiv:1812.10065 \[astro-ph.HE\]](#).
- [69] N. Giacobbo and M. Mapelli, *Mon. Not. Roy. Astron. Soc.* **480**, 2011 (2018), [arXiv:1806.00001 \[astro-ph.HE\]](#).
- [70] H.-Y. Chen, S. Vitale, and F. Foucart, *Astrophys. J. Lett.* **920**, L3 (2021), [arXiv:2107.02714 \[astro-ph.HE\]](#).
- [71] J. J. Cowan, C. Sneden, J. E. Lawler, A. Aprahamian, M. Wiescher, K. Langanke, G. Martínez-Pinedo, and F.-K. Thielemann, *Rev. Mod. Phys.* **93**, 15002 (2021), [arXiv:1901.01410 \[astro-ph.HE\]](#).
- [72] A. G. Abac *et al.* (LIGO Scientific, VIRGO, KAGRA), (2025), [arXiv:2508.18081 \[gr-qc\]](#).